Role of the martensitic microstructure in the stabilized residual stresses under cyclic loading and in the fatigue behavior of two steels

Dalenda Jeddi, Thierry Palin-Luc

Role of the martensitic microstructure in the stabilized residual stresses under cyclic loading and in the fatigue behavior of two steels

Dalenda Jeddi [a,*], Thierry Palin-Luc [b,c]

[a] University of Tunis El Manar- Department of Physics, IPEIEM, BP 244, 2092 Tunis, Tunisia
[b] Univ. Bordeaux, CNRS, Bordeaux INP, I2M, UMR 5295, F-33400 Talence, France
[c] Arts et Metiers Institute of Technology, CNRS, Bordeaux INP, HesamUniversite, I2M, UMR 5295, F-33400 Talence, France

Keywords:
Residual stress
Quenched martensite
Tempered martensite
Retained austenite
High cycle fatigue

A B S T R A C T

The influence of martensitic microstructure on the evolution of residual stresses during cyclic loading has been investigated using X-ray diffraction, both in martensite and in retained austenite. Different microstructures containing retained austenite fractions of 25% and 40% were obtained by vacuum carburizing applied to the 14NiCr11 steel. Additionally, other microstructures, such as quenched or tempered martensite of the 42CrMo4 steel were also studied.The results indicate that, for the same hardness and similar stabilized residual stresses in retained austenite, the greater the longitudinal residual stresses in quenched martensite, the greater the improvement in fatigue strength.From initial biaxial isotropic residual stresses, cyclic loading close to the endurance limit created anisotropic residual stress relaxation in quenched martensite and retained austenite. After cyclic loading, the longitudinal residual stresses were higher than the transverse residual stresses, regardless of the type of loading (bending in the case of 14NiCr11 carburized steel or combined bending and torsion in the case of the 42CrMo4 steel). The high level of longitudinal residual stresses after cyclic loading was correlated with the high retained austenite transformation to martensite in the case of 14NiCr11 carburized steel. The anisotropy of the stabilized residual stresses (after a few 10th of cycles) is due to the metastability of quenched martensite under cyclic loading.

1. Introduction

In the field of high cycle fatigue, it is well established that crack initiation mainly takes place at the surface of mechanical components. To address this issue, surface treatments are commonly employed on components experiencing high cycle fatigue loadings. These treatments aim to generate a surface layer with adequate hardness and compressive residual stresses, effectively delaying crack initiation and increasing the fatigue strength [1–3]. The presence of a ductile core further enhances the resistance to crack propagation and the impact toughness of the component [2]. Residual stresses, which are considered as mean stresses, play a key role in fatigue resistance [1,4,5].

Carburizing treatment of low alloy steels is a widely used surface treatment to improve fatigue resistance. Indeed, carburizing increases the surface hardness and creates a field of compressive residual stresses near the surface [6–13]. The residual stresses in carburized steels result from the superposition of two residual stress fields generated by the cooling process (thermal effect) and phase transformations (metallurgical effect) [14,15]. The delay in core cooling relative to the surface generates compressive residual stresses on the surface [7]. In addition, the carbon enrichment of the carburized layer delays martensitic transformation at the surface compared to the core, contributing to the formation of compressive residual stresses at the surface. This delay in phase transformation is attributed to the decrease in the martensite transformation temperatures (Ms and M_f) with increasing carbon content [7,12,14–17]. Thus, the core of specimens transforms before the surface during quenching. As carbon content increases toward the surface, volume expansion increases. While the surface would be expected to be the longest if it was free. However, it is not, because the adjacent material is constrained and therefore in compression. The martensitic transformation causes incompatible strain fields, generating varying internal stresses in both retained austenite and martensite [18]. But residual stresses and microstructural features of carburized layers exhibit instability under cyclic loading [19–29]. Qualitatively, the main microstructural cyclic instability concerns retained austenite, a metastable phase susceptible to phase transformation under external forces [30–38].

* Corresponding author.
E-mail address: dalenda.jeddi@ipeiem.utm.tn (D. Jeddi).

https://doi.org/10.1016/j.ijfatigue.2024.108168

Nomenclature

HV	Vickers microhardness
R	stress ratio
σ_a	bending stress amplitude
σ_{max}	maximum bending stress
τ_a	torsional (shear) stress amplitude
α	body centred cubic martensite
α'	centred tetragonal martensite
K_{tb}	theoretical stress concentration factor under bending loading
K_{tto}	theoretical stress concentration factor under torsion loading
σ_R	residual stress
σ^R_{long}	longitudinal residual stress
σ^R_{trans}	transverse residual stress
σ_D	endurance limit at 10^6 or 2×10^6 cycles depending on the investigated steel
γ_R	retained austenite
$R_{p0.2}$	yield stress under monotonic quasi-static tension
UTS	ultimate tensile strength

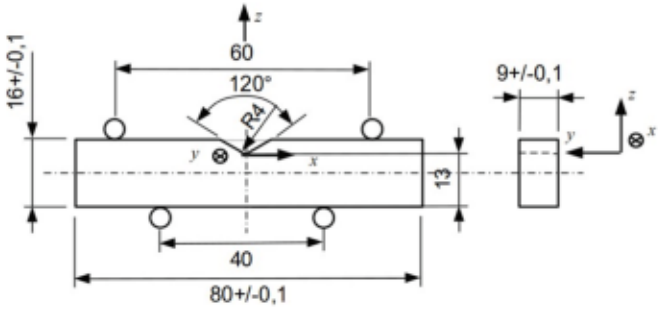

Fig. 2. Specimen geometry of the 14NiCr11 steel and location of rollers for the four points plane bending loading (R = 0.1) with Kt_b(bending) = 1.6, according to [60].

recommended for optimum hardening [9,12,51].

It has also been reported that there is a competition between the relaxation of compressive residual stresses under cyclic loading and their increase by transformation of retained austenite to martensite in the carburized layers [23,52]. In the particular case of bending fatigue the transformation of retained austenite to martensite under cyclic loading leads to an increase in the level of compressive residual stresses, which is beneficial for improving the fatigue strength of the carburized layers [43–56]. In addition, studies presented in [56,57] have shown

Table 1
Chemical compositions and mechanical properties under monotonic quasi-static tensile loading of 42CrMo4and 14NiCr11steels before the heat treatments of this study.

Chemical composition										Mechanical tensile properties		
Element (w%)	C	Si	Mn	P	S	Cr	Ni	Mo	Cu	UTS (MPa)	$R_{p0.2}$ (MPa)	Elongation (%)
14NiCr11	0.14	0.24	0.46	0.015	0.032	0.79	3.18	<0.02	0.22	553	408	30
42CrMo4	0.368	–	0.651	0.019	0.030	0.962	0.107	0.174	0.207	1050*	970*	16.5*

*from the literature [59] (the structure of the 42CrMo4 steel in reception state results from the oil quenching after austenisation at 850 °C and tempering at 580 °C during 1 h).

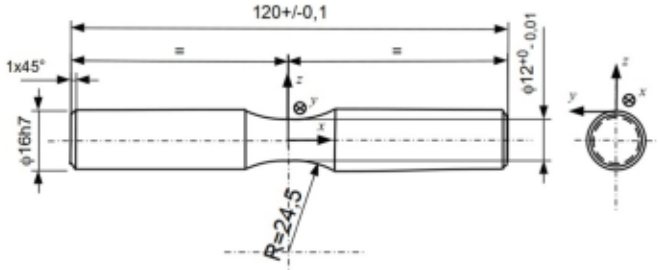

Fig. 1. Fatigue specimen for combined torsion (R = -1) and plane bending loading (R = -1) with $\frac{\sigma_a}{\tau_a} = 0.5$ of the 42CrMo4 steel (Kt_b (bending) = 1.07 and Kt_{to} (torsion) = 1.05, according to [60]).

In the literature, the role of retained austenite instability in fatigue life is occasionally controversial when based on its initial content. Some authors argue that the thermodynamic instability of the retained austenite under stress loading reduces the tensile and fatigue strength of carburized steels [34]. On the contrary, experimental results obtained by others show that the presence of retained austenite in carburized layers improves fatigue strength [39–43]. These controversial views are attributed to the different mechanisms of fatigue crack initiation and propagation [9,28,41,44–46], which depend on the type of cyclic loading, the volume fraction and morphology of retained austenite [43,46], the case depth [43,45,47], the austenite grain size [11,45,49–51], the surface residual stresses [43]. In general, a retained austenite content of 20–25 % in carburized layers of steels is

that the level of residual stresses depends not only on the rate of transformation of retained austenite into martensite under cyclic loading, but also on the crystalline structure of the martensite (α body-centered cubic (bcc) structure or α' centered tetragonal structure). It has been found that the higher the proportion of α' martensite, the higher the value of compressive residual stresses.

To sum up, carburized or carbon-infiltrated hardened layers are subject to gradients in microstructure, hardness and residual stresses. The transformation of retained austenite to martensite under cyclic loading produces changes in these gradients. Consequently, it would be more appropriate to keep as many variables as possible constant and to consider all of these expected changes in order to better understand their effect on the high cycle fatigue strength. In the present study, two vacuum carburizing treatments were performed on 14NiCr11 steel. To investigate the impact on the fatigue resistance of the microstructure gradient evolution during cyclic loading, specific vacuum carburizing parameters were chosen to produce two maximum levels of retained austenite in the surface layers: 25 % and 40 %. This allowed for a comparative analysis of the behavior of different microstructures under cyclic loading and an assessment of their influence on the stability of the residual stresses and fatigue resistance.

Given the coexistence of retained austenite with martensite in the case-hardened layers, the induced residual stresses resulting from these distinct structures were evaluated both before and after cyclic loading. This analysis was performed not only on martensite but also on retained austenite, which is relatively uncommon according to the authors' knowledge and represents a novel aspect of this study.

To differentiate between the influence of the austenite–martensite

Table 2
Vacuum carburizing conditions applied to notched fatigue specimens in 14NiCr11 steel.

Type of treatment		Carburizing temperature (°K)	Duration of carburization (s)	Temperature of preparing to the quenching (°K)	Duration (s)	Type of quenching
Type 1		1223	8460	1153	300	oil
Type 2	Cycle 1	1253	8460	1253	1860	oil
———	Cycle 2	1253	3120	1253	1800	oil

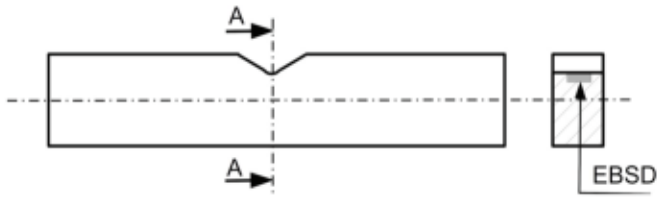

Fig. 3. Location of the area analyzed by EBSD on the carburized specimens in 14NiCr11.

Table 3
X–Ray diffraction parameters for the determination of the residual stresses.

	In martensite	In retained austenite
Radiation	K α Chrome	K α Chrome
Angle (2 θ°)	156	152
Wave length (A°)	2.2897	2.2897
X-Ray diffraction planes	{211}	{311}
Young Modulus(MPa)	210,000	210,000
Poisson coefficient	0.295	0.295
S_1 (MPa^{-1})	$-1.28x10^{-6}$	$-1.8x10^{-6}$
½ S_2 (MPa^{-1})	$5.83x10^{-6}$	$6.54x10^{-6}$

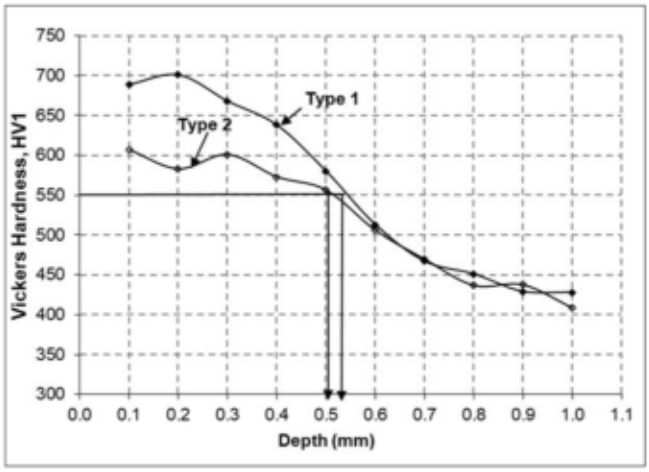

Fig. 4. Microhardness profiles resulting from type 1 and 2 carburizing treatments of the 14NiCr11 steel.

phase transformation under cyclic loading and the change of the martensitic microstructure on the cyclic evolution of residual stresses, alternative microstructures without retained austenite were also examined. These microstructures were obtained by applying quenching and tempering treatments to specimens in 42CrMo4 steel. It is worth noting that the quenched martensitic microstructure exhibits extremely low ductility, which has limited the utilization of martensitic steels as structural materials [58].Therefore, studying the behavior of this microstructure under cyclic loading is essential for understanding its impact on the evolution of the residual stresses observed during fatigue tests. Additionally, Electron Backscatter Diffraction (EBSD) analyses were conducted before and after loading to capture the microstructural changes occurring under cyclic loading.

2. Materials, treatments and tests

2.1. Materials

The materials investigated are the commercial low alloy steel 42CrMo4 and the steel 14NiCr11. Their chemical compositions and mechanical properties under monotonic quasi-static tensile loading are given in Table 1. The heat treatments of these steels are detailed in section 2.3.

2.2. Specimens preparation and treatments

The geometries of the specimens made of 42CrMo4 steel and those of 14NiCr11 steel are shown in Figs. 1 and 2. Two batches of fatigue specimens made of 42CrMo4 steel were prepared. After machining, a heating treatment at 880 °C for 30 mn and then quenching in oil was applied equally to both. This treatment was followed by tempering at 430 °C for 2 h for one batch, but nothing else to the other batch. Two types of vacuum carburizing treatments were applied to the notched fatigue specimens in 14NiCr11 steel. They aimed at obtaining two fractions of retained austenite in the hardened layers (Table 2). All treatments were carried out after machining (i.e. on the final specimen geometry).

- Type 1: this type of treatment is representative of the conditions commonly used in industry to limit the retained austenite fraction to 20 % or less, for fatigue performance reasons.
- Type 2: this treatment is aimed at obtaining a higher retained austenite fraction by selecting two treatment cycles, each time appropriately managing the propane flow in the furnace.

2.3. Characterization of the treated layers

2.3.1. Hardening and microstructure characterization

The surface hardening induced by the two types of carburizing treatments was evaluated by micro hardness tests under a load of 100 gf. The resulting metallurgical transformations were examined by optical microscope on transverse cross sections. Retained austenite fractions were determined by dispersive energy X-ray diffraction (DEXRD) [61]. EBSD analysis were carried out with a SEM FEG (JEOL JSM 7100F TTLS LV and an Oxford instrument EBSD detector) on a cross section located at the bottom of the notch of the specimens (Fig. 3). These samples were polished by vibration with OPS(during 40 min).

2.3.2. Analysis of the residual stresses

Residual stress gradients in the longitudinal and transverse directions before and after cyclic loading were determined by X-ray diffraction under the conditions given in Table 3. These analysis were carried out at the bottom of the notch for the 14NiCr11 specimens and at the bottom of the median torus for the 42CrMo4 specimens. A circular X-Ray beam spot with a diameter of 2.5 mm was used. To avoid the effects of curvature in the longitudinal direction of the specimens, lead masks were used to limit the impact of the X-ray beam. The position of the diffraction peaks was determined using the barycentre-centred method developed by CETIM. To produce the in depth residual stress profiles, the material was removed by local nitric dissolution, and the metrological control of each removal was performed using a profilometer. The

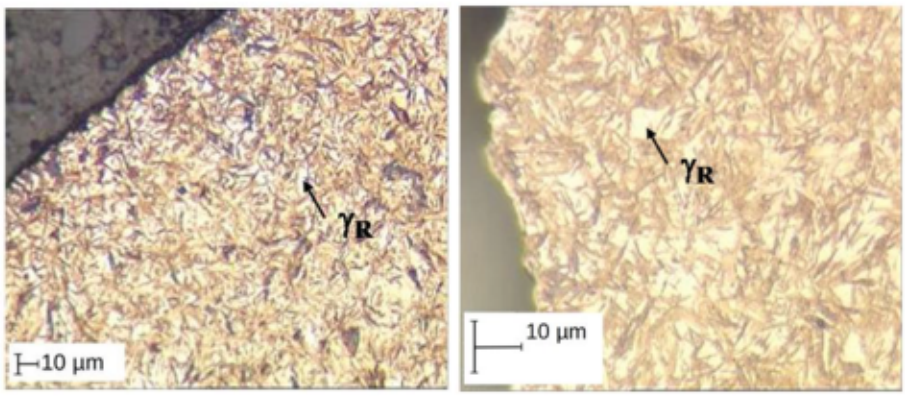

-a- -b-

Fig. 5. Martensite and retained austenite microstructure after vacuum carburizing of the 14NiCr11 steel (retained austenite in white color and martensite in dark), a) Type1, b) Type 2.

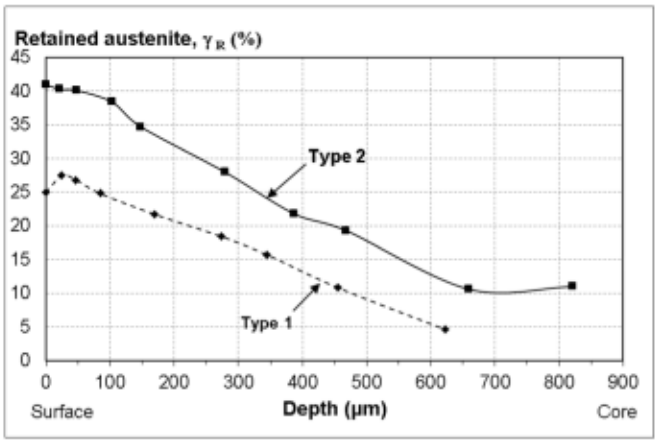

Fig. 6. Retained austenite profiles in the carburized layers of the 14NiCr11 steel before cyclic loading.

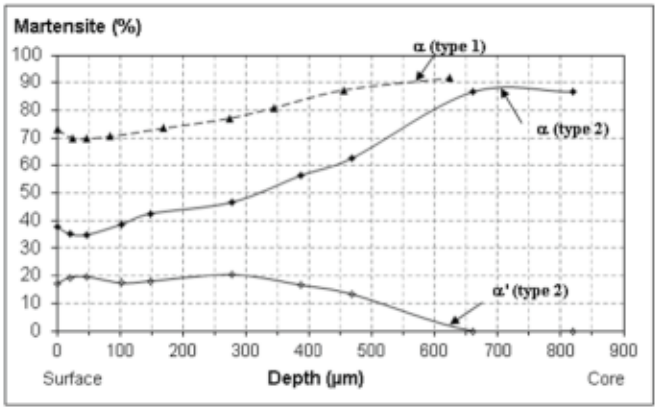

Fig. 7. Martensite profiles in the carburized layers of the 14NiCr11 steel before cyclic loading.

residual stresses have not been corrected by the Moore and Evans technique [62] or any other method to take account of the removed volume of the material by electrolytic polishing. Residual stresses are given in the (x, y, z) coordinate system illustrated in Figs. 1 and 2 so that ($\sigma_{long} = \sigma_{xx}$ and $\sigma_{trans} = \sigma_{yy}$).

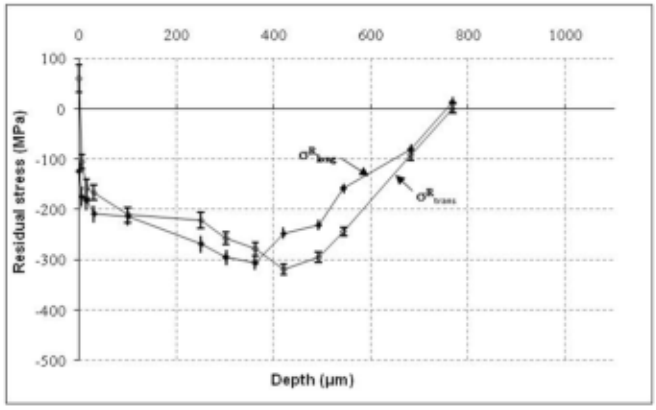

- a -

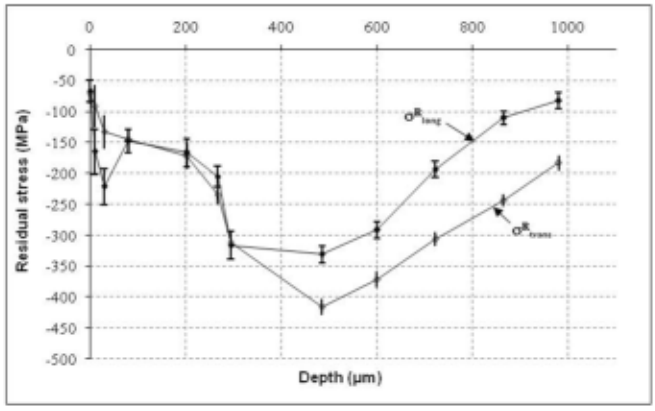

- b -

Fig. 8. Residual stresses profiles in martensite of the 14NiCr11 carburized steel before cyclic loading, a) Type1, b) Type2.

2.3.3. *Fatigue tests*

The 42CrMo4 steel specimens were subjected to fully reversed plane bending combined with fully reversed torsion, both in phase, with a stress amplitude ratio $\sigma_a/\tau_a = 0.5$, at a frequency of 50 Hz. The tests were carried out on the LLS machine atI2M Bordeaux [63]. Specimens of 14NiCr11 steel were subjected to four point plane bending fatigue tests

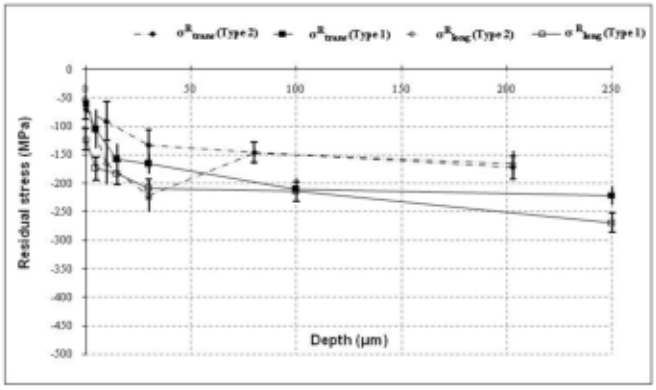

Fig. 9. Zoom on the gradients of residual stresses profiles in martensite, resulting from the carburized treatments of the 14NiCr11steel before cyclic loading.

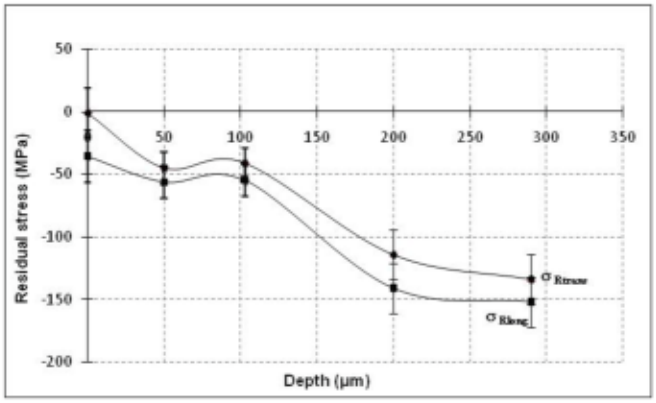

Fig. 10. Residual stresses versus depth in the quenched martensite of the 42CrMo4 steel before cyclic loading.

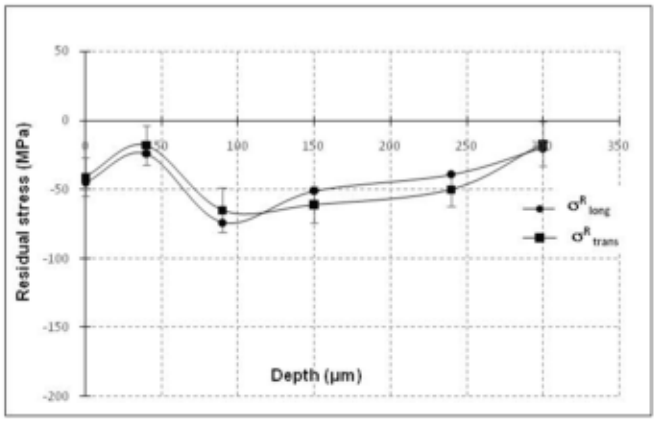

Fig. 11. Residual stresses versus depth in the quenched and tempered martensite of the 42CrMo4 steel before cyclic loading.

with a stress ratio of R = 0.1 and a frequency of 20 Hz. For these two steels, the endurance limits were determined by the staircase method at 10^6or 2×10^6 cycles respectively.

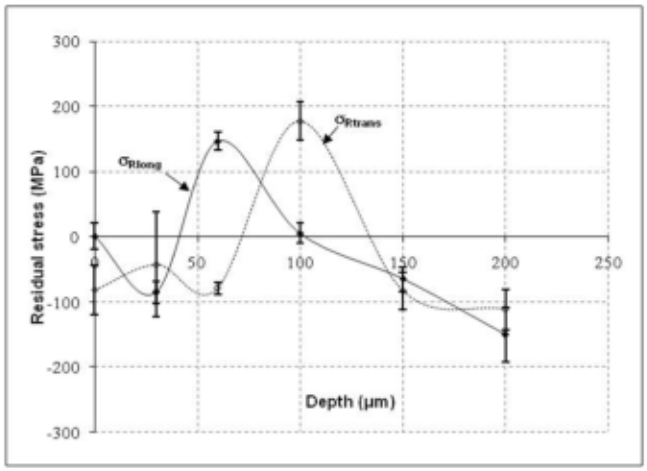

- a -

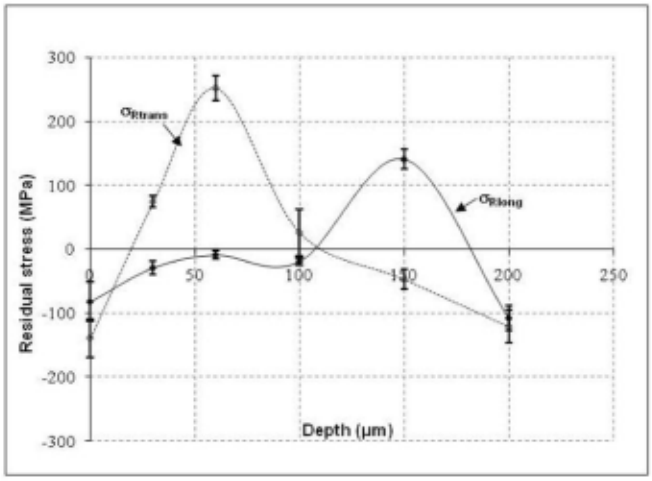

- b -

Fig. 12. Residual stresses in the retained austenite of the carburized 14NiCr11 steel before cyclic loading, a) type 1, b) type 2.

3. Results

3.1. Microstructure before cyclic loading

The microhardness profiles of the 14NiCr11 steel indicate an identical conventional case depth of approximatively 0.5 mm, induced by the two carburizing treatments (Fig. 4). The Type 1 treatment consistently results in a greater level of hardening compared to the type 2 treatment in the treated layers. The surface microstructure reveals more austenite in the case of the Type 2 treatment, as depicted in Fig. 5.

A quantitative analysis of the DEXRD spectrum reveals several observations:

- Retained austenite quantification demonstrates a gradient of this phase from the surface to the core of the specimen.
- The fractions of retained austenite obtained after the type 2 treatment are more important than those obtained after the type 1 treatment, for the same depth of treated layers.
- The maximum fraction of retained austenite increases in the upper surface of the specimens. It is approximately 25 % and 41 % for Type 1 and Type 2 treatments respectively (Fig. 6).
- In the case of the Type 2 treatment, two forms of martensite coexist, martensite α (body-centered cubic (bcc) structure) and α ' (centered tetragonal structure), with a predominance of the structure α (up to 0.5 mm). The treated layer corresponding to the Type 1 treatment consists

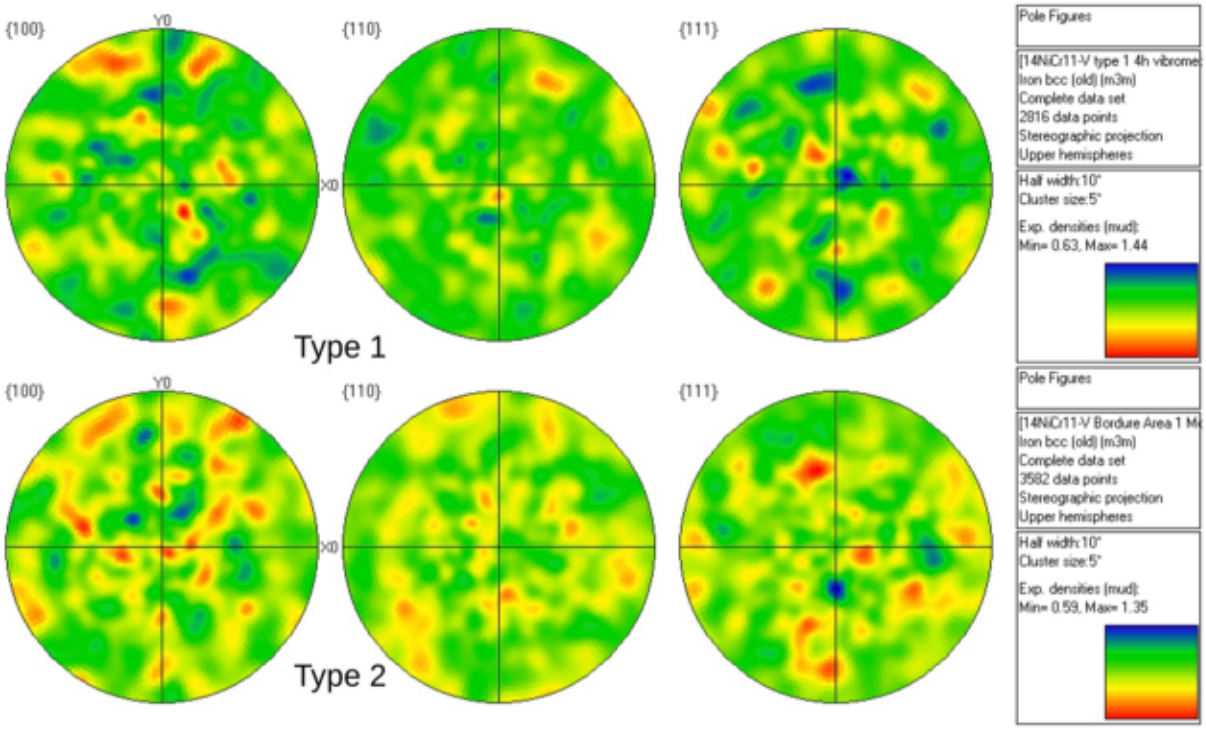

- a -

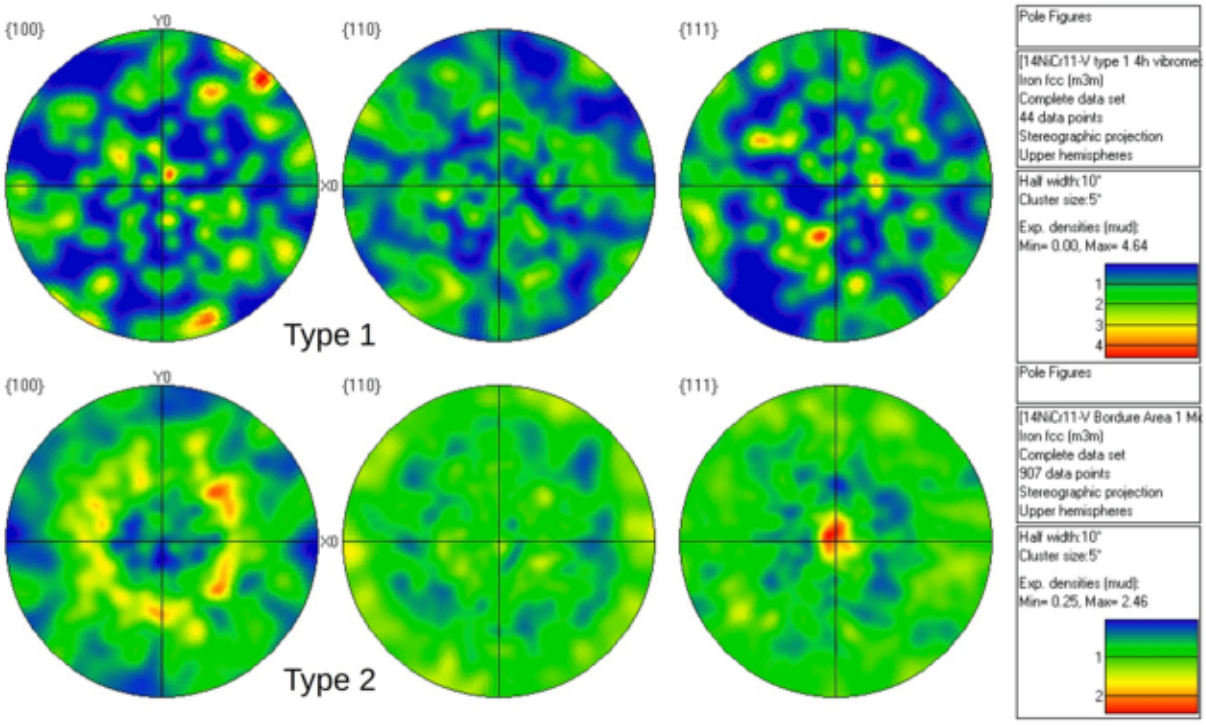

- b -

Fig. 13. EBSD analysis of carburized 14NiCr11 steel before cyclic loading a) martensite, b) retained austenite.

exclusively of martensite α form, as illustrated in Fig. 7. In both cases, the microstructure of the treated layers is made up of martensite, austenite and carbides. Microstructure of 42CrMo4 is fully martensitic for the two batches.

3.2. Residual stresses before cyclic loading

Residual stress profiles measured in the bottom of the notch of the 14NiCr11 fatigue specimens before cyclic loading, demonstrate a state of quasi biaxial (i.e. isotropic in the plane) compression in the martensite of the carburized layers for the two types of treatments (Fig. 8). In

Table 4
Fatigue strengths of the 42CrMo4 and the 14NiCr11 steels.

Material	Treatment	Loading type	K_t	R	Run outs	Frequency (Hz)	$^*\Delta\sigma_D/2$ (MPa) (bending)
42CrMo4	Quenched	Combined bending and torsion	$K_{tb} = 1.07$	−1	$2x10^6$	50	171
	Quenched & Tempered		$K_{ttso} = 1.05$	−1			197
14NiCr11	none	4 points bending	$K_{tb} = 1.6$	0.1	10^6	20	335
	Carburized Type 1						542
	Carburized Type2						595

$^*\Delta\sigma_D/2 = K_{tb}\ (\sigma_{max}\text{-}\sigma_{min})/2$.

Table 5
Carburized layers properties and fatigue strength of the 14NiCr11 steel.

State	Carburized layers properties	Type 1	Type 2
Before loading	γ_R (%) at the surface (z = 0)	25	41
	σ_R (MPa)	−260	−205
	$HV_{surface}$ (HV0.1)	700	606
	e (mm)	0.5	0.55
After 10^6 cycles of loading close to endurance limit	γ_R (%)	19	32
	Mean value of surface stabilized σ_R in quenched martensite(MPa)	≈-300	≈-400
	Mean value of surface stabilized σ_R in retained austenite (MPa)	−250	−250
	$HV_{surface}$ (HV0.1)	735	744
	$(\Delta\sigma_D/2)$(MPa)	542	595
Relative fatigue strength improvement at 10^6 cycles (%)		62	78

addition, martensite is a metastable interstitial solid solution of carbon in iron. It has a bcc structure at low carbon concentrations α. When the carbon concentration is higher; it causes the lattice to become distorted. A distortion that becomes more pronounced the higher the carbon content of the steel and the martensite has a centered tetragonal structure α'. This explains the higher level of compressive residual stresses in martensite for the same retained austenite content (i.e. The same carbon content) in the case of the Type 2 treatment, which resulted in a mixed structure of α (body-centered cubic (bcc) structure) and α' (centered tetragonal structure) compared to the Type 1 treatment.

The refined gradients in the first 200 μm from the surface indicate that the two types of treatments result in comparable residual stress profiles (Fig. 9).

The residual stresses analyzed before cyclic loading both in the quenched 42CrMo4 steel (Fig. 10) and in the quenched and tempered 42CrMo4 steel (Fig. 11) indicate compressive residual stresses. For the same depth, the residual stresses obtained after quenching are higher than those obtained after tempering. Indeed, during the tempering, the carbon supersaturation of the quenched martensite decreases through carbon expulsion, and the associated volume change leads to a relaxation of residual stresses compared to the untempered state [64].

To gain a better understanding of the evolution of the residual stresses during fatigue loading, residual stress profiles were analyzed in the austenite of the carburized 14NiCr11 steel. The obtained profiles are characterized by a highly random distribution from one measurement point to another, in both longitudinal and transverse directions (Fig. 12). This is likely due to the role of residual stresses in the grains at levels II and III, resulting from a heterogeneous microstructure at a smaller scale.

3.3. EBSD analysis before cyclic loading

Regarding the 14 NiCr11 steel, the pole figures obtained through EBSD analysis before fatigue loading reveal homogeneous martensitic structure at the surface for the two types of carburizing treatments.

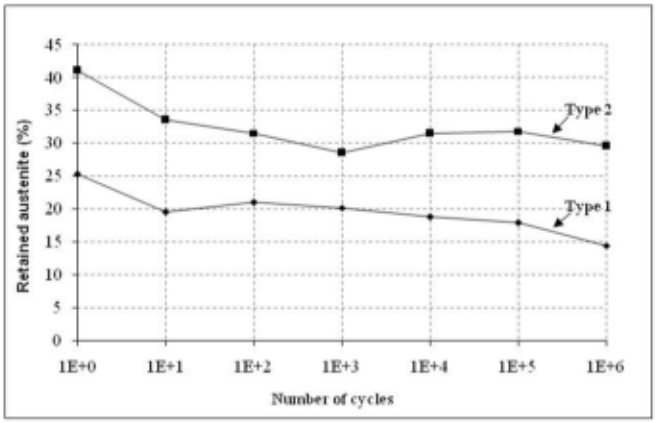

- a -

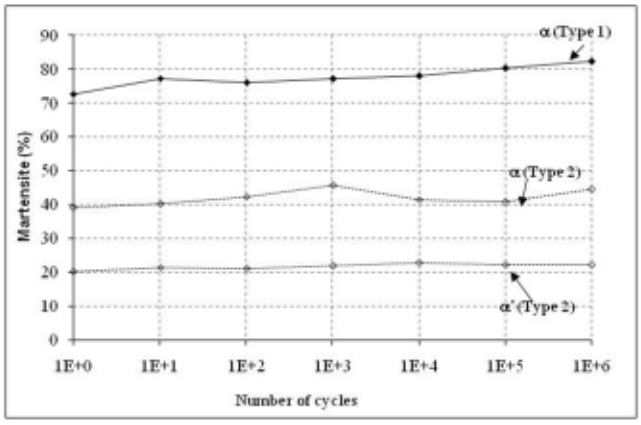

- b -

Fig. 14. Variations of the surface a) retained austenite and b) martensite fractions in the carburized layers of the 14NiCr11 steel as a function of the number of cycles during loading close to the fatigue limit (σ_{max} = 90 % σ_D). Each point corresponds to one specimen. The measurements were carried out at the bottom of the notch (at the surface).

(Fig. 13a). However, in the case of the Type 2 treatment which results in a surface retained austenite of 40 %, a small retained austenite texture is observed before cyclic loading (Fig. 13b). On the other hand, due to the absence of retained austenite and the fine microstructure of the martensite, EBSD analysis for the 42CrMo4 steel did not provide any significant information.

3.4. Fatigue strength

The experimental median values of the fatigue strengths according to the staircase method are shown in Table 4.

The characteristics of the carburized layers of the 14NiCr11 steel and their fatigue strengths are summarized in Table 5. It can be observed that the initial gradient of the properties before loading does not explain

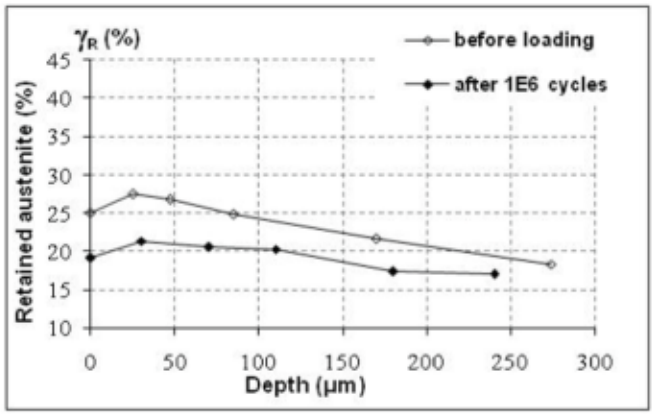

- a -

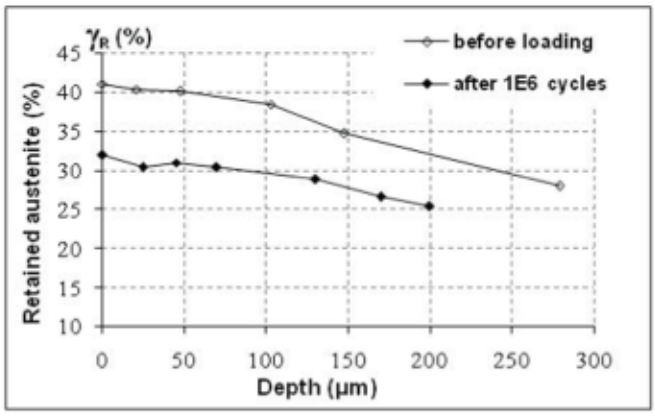

- b -

Fig. 15. Evolution of the retained austenite profilesin the carburized layers of the 14NiCr11 steel after 10^6cycles under loading close to the fatigue limit (σ_{max} = 90 % σ_D), (a) Type 1, (b) Type 2.

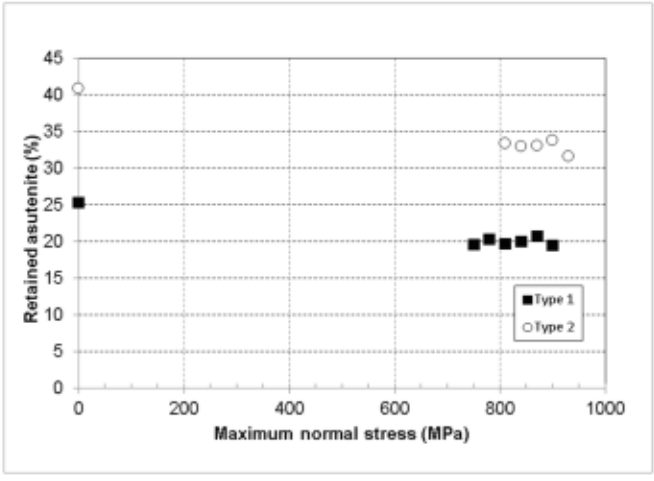

Fig. 16. Variations of the surface retained austenite fraction,γ_R, in the carburized layers of the 14NiCr11 steel as a function of the maximum applied stress (slightly higher than σ_D) after 10 loading cycles under plane bending (R = 0.1).

the obtained results. In fact, the literature suggests that higher hardness and compressive residual stress result in better fatigue improvement. Therefore, it was expected that the Type 1 treatment, which resulted in the highest hardness gradient and similar compressive residual stress, would provide better fatigue resistance. However, the opposite occurred, that is the reason why micostructural investigations have been carried out. They are presented in the next section.

3.5. Changes of the microstructure and the residual stresses under cyclic loading

3.5.1. Modification of the microstructure under cyclic loading

Retained austenite is a metastable phase that could transform into martensite under deformation. Even if the fatigue loading is lower than the macroscopic elastic limit, the austenite could be transformed by local microplasticity [41,65]. Therefore, we focused only on the microstructure transformation under cyclic loading of the carburized 14CrNi11 steel. We assume that the martensite microstructure of the 42CrMo4 steel remains the same at the grain scale because no microscope observations show the opposite.

It should be noted that the changes in microstructure and residual stresses under cyclic loading were observed on several specimens loaded differently as necessary. Measurements were taken on different specimens. Each specimen was loaded with a given stress and to a given number of cycles, then removed from the fatigue testing machine and analyzed (ex-situ measurement). These analysis were carried out at the bottom of the notch and at the surface. The results show that retained austenite transforms to bcc martensite during cyclic loading close to the endurance limit for both types of treatments (Fig. 14). Almost all of this transformation occurs during the first ten cycles. After 10^6 cycles, this transformation appears to be particularly localized in the first two hundred micrometers. The proportions of transformation are 5 % for the type 1 treatment and 10 % for the type 2 treatment on the entire unstable area (200 to 300 µm) (Fig. 15). Moreover, the results of the measurement of the retained austenite fraction at the surface, according to the applied stress, reveal the existence of a threshold fraction of retained austenite cyclically unstable (20 to 25 % of the initial fraction) (Fig. 16).It may be assumed that the transformation of retained austenite to martensite under cyclic loading close to endurance limit increases the local yield stress. Consequently, a steady-state is reached and no further transformation occurs under higher level of external applied stresses. Additional investigations should be carried out to try to understand this phenomenon.

The effect of these transformations on the changes in hardening, in the bottom of the notch during cyclic loading, does not affect the entire carburized layer for both types of treatments. However, for the Type 1 treatment, there is a more pronounced additional hardening up to a thickness of 300 µm compared to the Type 2 treatment (Fig. 17).

3.5.2. Redistribution of the residual stress fields during cyclic loading

a- Changes of the residual stresses in martensite.

- Carburized 14NiCr11 steel

The results show that after loading close to the endurance limit at 10^6 cycles, there is a redistribution of residual stresses in the two directions for the carburized 14NiCr11 steel (Fig. 18). The observed levels of stabilized residual stresses on the top surface are more significant in the longitudinal direction. For the type 2 treatment, the stabilized compressive residual stresses in depth (σ_{long} = − 400 MPa and σ_{trans} = − 150 MPa) are higher (in absolute value) than those of the type 1 treatment (σ_{long} = − 300 MPa and σ_{trans} = − 100 MPa). These values are related to the retained austenite fraction transformed into martensite by cyclic loading (5 % for type 1 whereas 10 % for type 2 treatment). The higher this fraction, the higher the stabilized compression levels are (Table 5). The same observations explain the increase in compressive

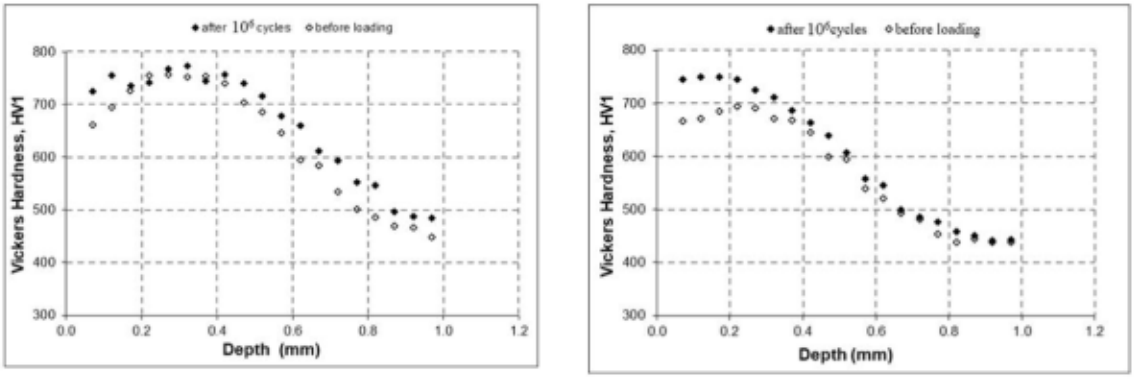

Fig. 17. Vickers hardness versus depth illustrating cyclic hardening of the carburized layers of the 14NiCr11 steel, (a) Type 1, (b) Type 2.

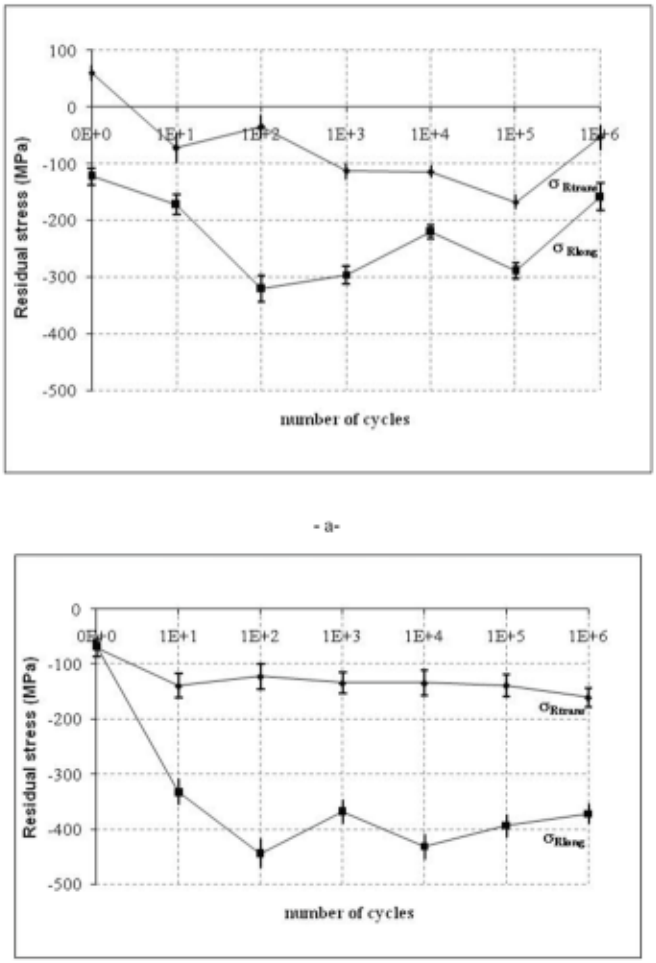

Fig. 18. Evolution of the surface residual stresses in martensite in the carburized layers of the 14NiCr11steel during loading close to the fatigue limit (σ_{max} = 90 % σ_D), a) Type 1, b) Type 2.

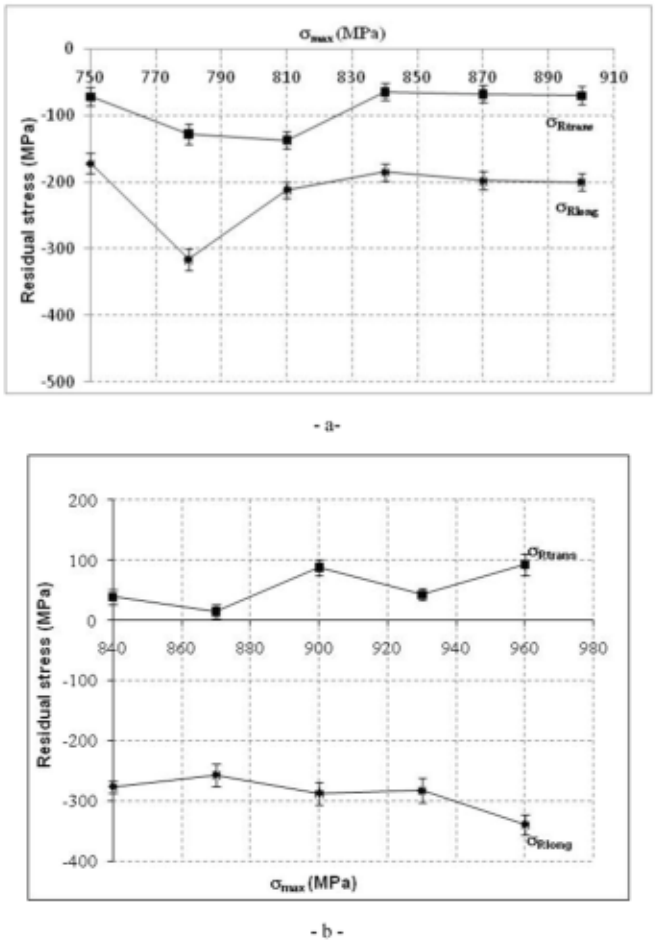

Fig. 19. Evolution of the surface residual stresses in martensiteinthe carburized layers of the 14NiCr11 steel as a function of the applied stress after 10 cycles of loading.

residual stresses at the surface after ten cycles of loading with applied stresses higher than the fatigue limit (Fig. 19).

- Quenched and tempered 42CrMo4 steel

The residual stresses after loading close to the endurance limit show a redistribution of the residual stresses in the two directions for the quenched 42CrMo4 steel specimens (Fig. 20-a). The levels of the stabilized residual stresses on the upper surface are more significant in the longitudinal direction than in the transverse one (σ_{long} = -200 MPa and σ_{trans} = -50 MPa). However, for the 42CrMo4 quenched and tempered steel, the residual stresses after loading close to the fatigue limit show a slight relaxation in both directions (Fig. 20-b).

The comparison between the different residual stress profiles in martensite after loading (for the carburized 14NiCr11 as for the quenched 42CrMo4) shows an anisotropy of the residual stresses in the

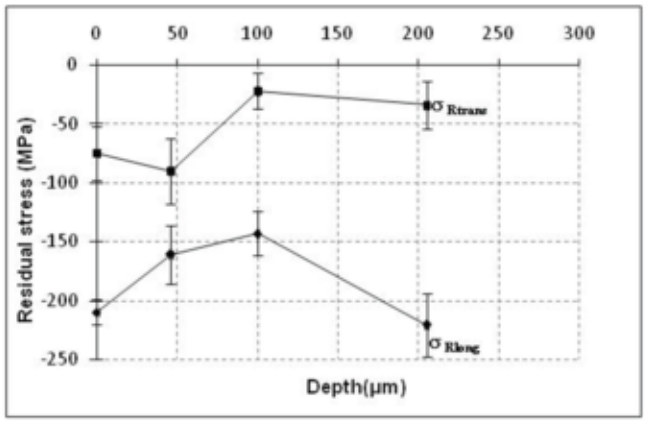

- a -

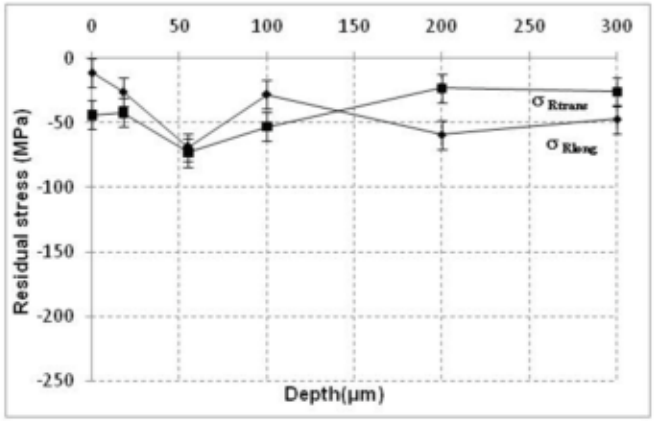

- b -

Fig. 20. Evolution of the residual stresses profiles in: a- quenched martensite and b- quenched and tempered martensite of the 42CrMo4 steel after 10^6 cycles under loading close to the fatigue limit (σ_{max} = 90 % σ_D).

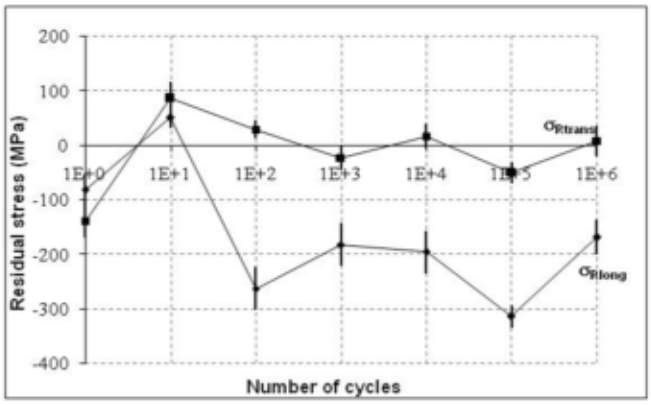

- a -

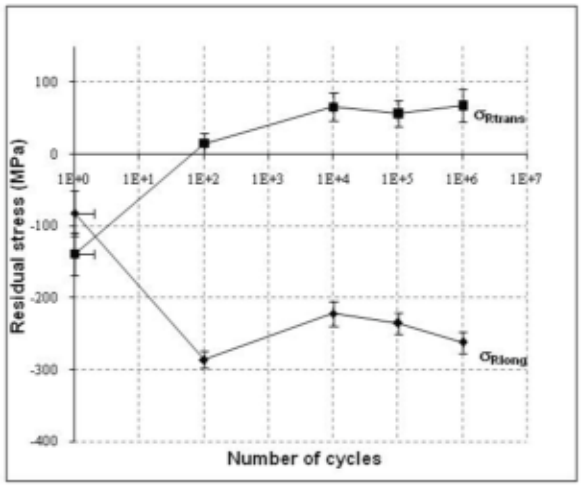

- b -

Fig. 21. Evolution of the surface residual stresses in retained austenite in carburized layers of the 14NiCr11 steel during cyclic loading close to the fatigue limit (σ_{max} = 90 % σ_D), a) Type 1, b) Type 2.

quenched martensite microstructure. In fact, they are more significant in the longitudinal direction than in the transverse direction. However, in tempered martensite there is a slight relaxation in both directions.

b- Changes of the residual stresses in the retained austenite.

Similarly, the compressive residual stresses in the austenitic phase are more significant in the longitudinal direction under cyclic loading (Fig. 21). The stabilized longitudinal residual stresses in retained austenite are close to −250 MPa in both cases of Type 1 and Type 2 carburizing treatments, despite the different levels of the residual stresses in martensite.

The surface residual stresses in retained austenite as a function of the loading amplitude are stabilized beyond the fatigue limit amplitude. Specifically, at 780 MPa for Type 1 and 840 MPa for Type 2 treatment (Fig. 22).

3.5.3. EBSD analysis after cyclic loading

After cyclic loading, the pole figures reveal a homogeneous structure of martensite and retained austenite (Fig. 23). It is noteworthy that the retained austenite from the Type 2 carburizing treatment loses its original texture during fatigue loading at a stress level close to the endurance limit (σ_{max} = 90 % σ_D).

4. Discussion

The results indicate that there is instability in the microstructure and residual stresses under cyclic loading. Therefore, the initial gradient of properties before loading does not explain the fatigue strength obtained for the 14NiCr11 carburized steel. In fact, the Type 1 treatment, which had the highest hardening gradient and similar compressive residual stresses to the Type 2 treatment, was expected to provide better resistance, while the opposite occurred.

It is well known that martensitic transformation is based on spontaneous cooperative shear motion. In metastable austenite, the necessary shear movement can be induced by externally applied mechanical loads [31]. As a result, the carburized layers of 14NiCr11 steel, which consist of retained austenite and quenched martensite undergo transformation under cyclic loading. Measurements demonstrate that this transformation occurs from the first cycles, regardless of the stress level, whether it is lower (90 %) or higher up to the fatigue limit. Furthermore, there is additional hardening in all unstable layers (200 to 300 µm) and a threshold fraction of retained austenite cyclically unstable (20 to 25 % of the initial fraction).

EBSD analysis on 14NiCr11 indicates that the austenite texture is lost due to austenite–martensite transformation caused by microplasticity under cyclic loading. The consequence of the microstructure instability under cyclic loading is the change of residual stresses compared to their values before cyclic loading close to the endurance limit. One notes that residual stresses in quenched martensite and retained austenite are unstable under cyclic loading. Despite comparable initial residual stress fields in the first 200 µm in the carburized layers, the levels reached after

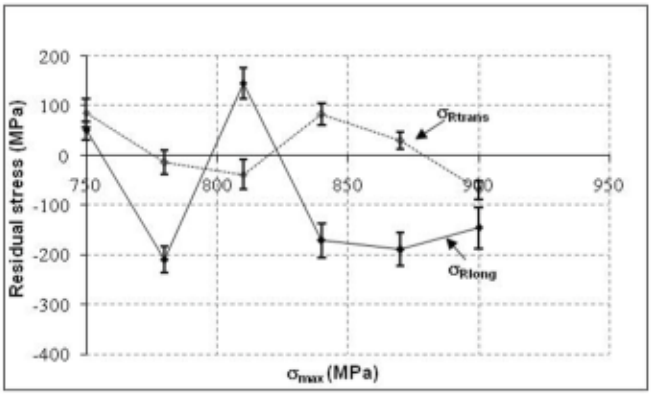

- a -

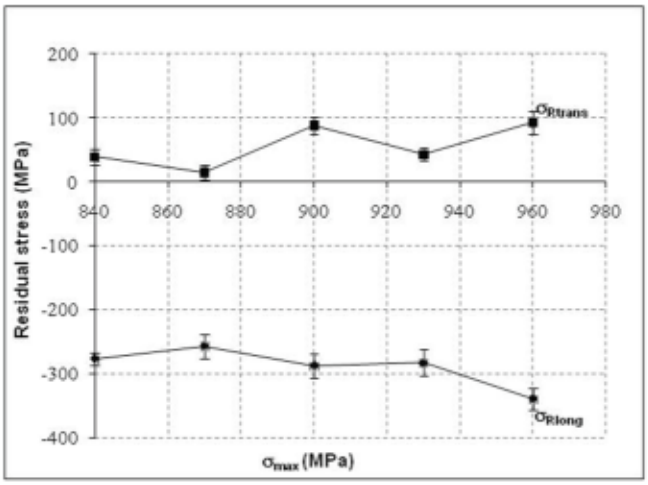

- b -

Fig. 22. Evolution of the surface residual stresses in retained austenite as a function of the applied maximum stress after 10 cycles on the 14NiCr11 carburized steel, a) Type 1, b) Type 2.

cyclic loading are determined by the transformed fraction of retained austenite to martensite. The higher this fraction is, the higher the stabilized compressive levels become.

The comparison of the stabilized properties of the carburized layers (Table 5) shows that the greater improvement of fatigue strength, the higher the fraction of retained austenite transformed during cyclic loading. Indeed, in the case of the type 1 treatment, the fatigue improvement is about 62 %, only 5 % of retained austenite has been cyclically transformed into martensite, resulting in stabilized surface residual stress levels (in the martensite) of approximately −300 MPa. In contrast, the carburized layer obtained by treatment 2 offers a relatively greater improvement (78 %), due to a higher fraction of cyclically transformed retained austenite (10 %), resulting in more significant level of stabilized compressive residual stresses at the surface, approximately −400 MPa. The level of stabilized surface hardening achieved at the extreme surface is quite comparable for both treatments, around 740 HV0.1. The level of stabilized residual stresses in the retained austenite after cyclic loading remains around −250 MPa for both treatments. Regardless of the retained austenite fraction before loading or transformed during fatigue loading, both cases of carburizing treatment applied to the 14NiCr11 steel exhibit instability and anisotropy of the residual stresses after fatigue loading. Specifically, higher compressive values were observed in the longitudinal direction than in the transverse one.

The same phenomenon of instability and anisotropy of the residual stresses after cyclic loading is observed in the case of the quenched 42CrMo4 steel under combined torsion and plane bending loading. But not in the case of the quenched and tempered 42CrMo4 steel, where the residual stresses remain isotropic before and after cyclic loading.

The anisotropy of the residual stresses between the longitudinal and transverse directions after cyclic loading is a phenomenon observed across different types of steels, treatments, and loading conditions (bending or combined torsion and bending). Since the two investigated steels in this study contains different austenite volume fractions (there is no austenite in 42CrMo4), the anisotropy of the residual stresses cannot be attributed to austenite transformation under cyclic loading. The only common feature among the different structures studied in this paper, is the presence of quenched martensite. Furthermore, the absence of this phenomenon in the case of tempered 42CrMo4 steel suggests that quenched martensite present in both 14NiCr11 and 42CrMo4 steels is responsible for the anisotropy of residual stresses after fatigue loading. Additional investigations are needed to deeper analyze and understand this phenomenon.

Since the results of this study suggest that quenched martensite present in both 14NiCr11 and 42CrMo4 steels is responsible for the anisotropy of residual stresses after fatigue loading, the authors think that knowing the macroscopic yield stress of the steel is not the key point for understanding and then modelling this phenomenon. For a deeper understanding of the residual stress redistribution in a future study, the authors suggest to characterize the cyclic yield stress of the carburized 14NiCr11 steel at different depths, i.e. with different microstructures. Indeed in this study, this material is surface-treated consequently there is a microstructure heterogeneity from the surface to the core. However, such tests are difficult to be carried out because it is needed to manufacture and then test very small specimens or to do cyclic mechanical tests on micro-pillars. For the 42CrMo4 steel, it should be needed to know the cyclic yield stress of both quenched martensite and tempered martensite phases under different loading ratios for being able to model and simulate the cyclic behavior of specimens by finite element analysis in a future study.

5. Conclusion and prospects

In summary, the results of this study show that the instability and anisotropy of the residual stresses after cyclic loading are observed in both carburized 14NiCr11 and quenched 42CrMo4 steels. The transformation of retained austenite to martensite under cyclic loading causes an additional hardening in unstable layers and leads to a threshold fraction of retained austenite that is cyclically unstable. This instability results in a relaxation of the residual stresses and higher compressive values in the longitudinal direction than in the transverse direction. The study also highlights the importance of the stabilized residual stresses in the martensite microstructure for the high cycle fatigue strength of steels.

The results suggest that the metastable quenched martensite in both 14NiCr11 and 42CrMo4 steels is responsible for the residual stress anisotropy after cyclic loading, rather than the transformation of retained austenite to martensite. To confirm this hypothesis, the authors suggest that further investigations at the dislocation and precipate scale would be required.

Furthermore, the results of this study would be useful for simulating, at the microstructure scale, the effects of surface heat treatments on the high cycle fatigue strength of steels. Coupling polycristal plasticity and phase transformation should be useful to do that.

Declaration of competing interest

The authors declare that they have no known competing financial interests or personal relationships that could have appeared to influence the work reported in this paper.

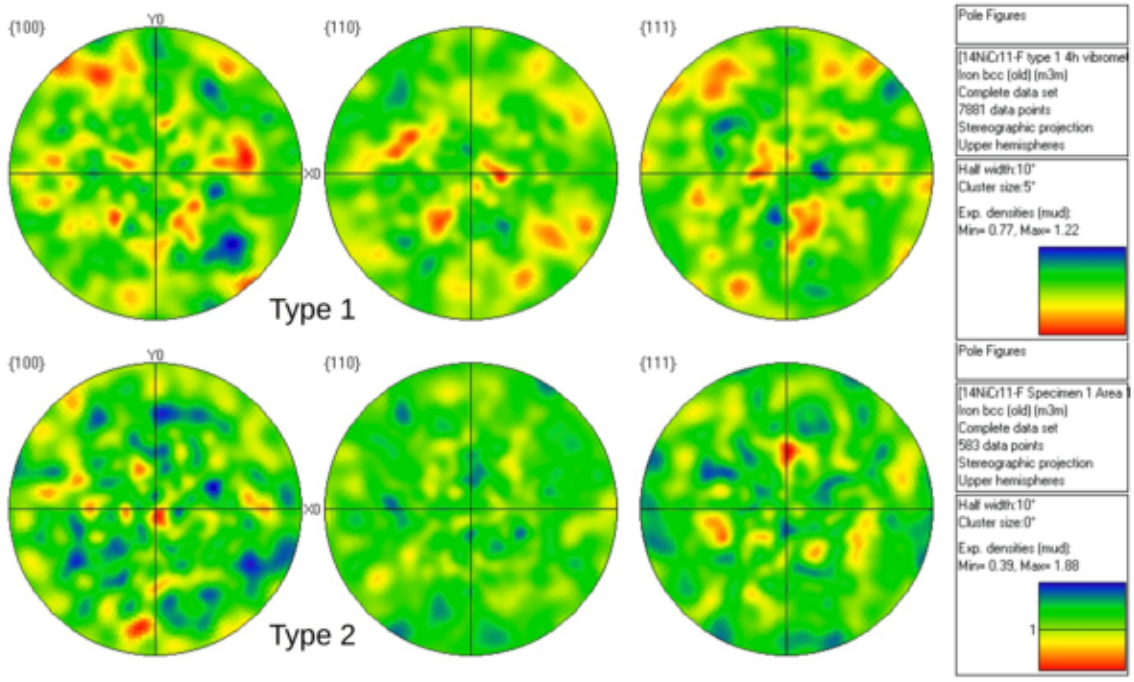

- a -

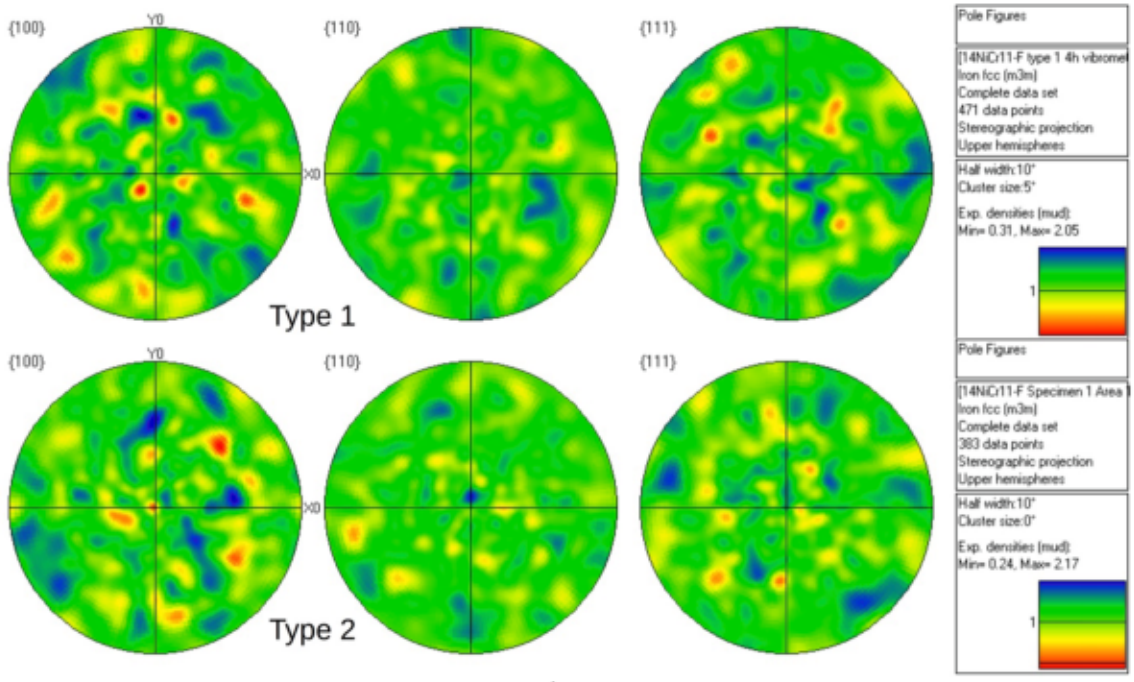

- b -

Fig. 23. EBSD analysis of the carburized 14NiCr11 steel after cyclic loading close to the fatigue limit (σ_{max} = 90 % σ_D), a) retained austenite, b) martensite.

Data availability

Data will be made available on request.

References

[1] Palin-luc T, Coupard D, Dumas C, Bristiel P. Simulation of the multiaxial fatigue strength of steel component treated by surface induction hardening and comparison with experiments. Int J Fatigue 2011. https://doi.10.1016/j.ijfatigue.2011.02.004.

[2] Schjive J. Fatigue of Structures and Materials, Springer; 2009. ISBN: 978-1-4020-6807-2.

[3] Bathais C, Pineau A. Fatigue of Materials and Structures: Fundamentals. ISTE, https://doi.10.1002/9781118623435.

[4] Crossland B. Int. IME/ASME, London: Conf. Fatigue Met; 1956.

[5] Skally N, Flavenot JF. Les contraintes résiduelles, attention elles se relaxent. CETIM Inform 1985;90:35–47.

[6] Varol R. Effect of heat and mechanical surface treatments on the fatigue properties of SAE 8620 steel. Metall 1996;50(N° 4) 257–259.
[7] Ebert LJ. The role of residual stresses in the mechanical performance of case carburized steels. Metall Trans A 1978. https://doi.org/10.1007/BF02661936.
[8] Km HJ, Kweon YG. High cycle fatigue behavior of gas-carburized medium carbon Cr-Mo steel. Metall Mater Trans A 1996;27A. https://doi.org/10.1007/BF02652349.
[9] Szpunar E, Bielanik J. Influence of retained austenite on propagation of fatigue cracks in carburized cases of toothed elements. Heat Treatment 1984;84:39.1–39.9.
[10] Jeong B, Kato M, Inoue K, Takatsu N. The bending strength of carburized fine module gear teeth. JSME Int J Series 1992;III. https://doi.org/10.1299/jsmec1988.35.136.
[11] Larsson M, Ölund P, Blom R, Waburger H, Melander A, Preston S. Fatigue properties after carburising: influence of core hardness and notch geometry on fatigue properties of case hardened steels. Scandinav J Metall 1994;23:62–73.
[12] Krauss G. Microstructure and performance of carburized steel: part II. Adava Mater Process 1995. n° 7, p.48U-48Y.
[13] Panhans MA, Fournelle RA. High cycle fatigue resistance of AISI E9310 carburized steel with two different levels of surface retained austenite and surface residual stress; 1981. 10.1007/BF02833074.
[14] Parrish G, Harper GS. Production Gas Carburising. U.K.: Pergamon Press Ltd; 1985. p. 64–73.
[15] Boyle E, Northwood DO, Bowers R, Sun X, Bauerle P. Microstructural effects on residual stress, retained austenite, and case depth of carburized automotive steels. SAE Int J Mater Manufact 2009;1(1):697–708.
[16] Liu Y, Qin S, Hao Q, Chen N, Zuo X, Rong Y. Finite element simulation and experimental verification of internal stress of quenched AISI 4140 cylinders[J]. Metall Mater Trans A 2017;48:1402–13. https://doi.org/10.1007/s11661-016-3916-6.
[17] Yang Q, Ren X, Gao Y, Li Y, Zhao Y, Yao M. Effect of carburization on residual stress field of 20CrMnTi specimen and its numerical simulation. Mater Sci Eng A 2005;392(1-2):240–7.
[18] Papula S, Talonen J, Hänninen H. Effect of residual stress and strain-induced a ε-martensite on delayed cracking of metastable austenitic stainless steels. Miner Met Mater Soc ASM Int 2013. https://doi.org/10.1007/s11661-013-2090-3.
[19] da Silva VF, Canale LF, Spinelli D, Bose-Filho WW, Crnkovic OR. Influence of retained austenite on short fatigue crack growth and wear resistance of case carburized steel. J Mater Eng Perform 1999;8(5):543–8.
[20] Asami K, Emura H. Fatigue strength characteristics of high-strength steel. JSME Int J Series 1990;33(3):367–74.
[21] Hauk V, Hougardy HP, Macherauch E, Tietz H-D. Influence of residual stresses on fatigue crack growth behaviour of case-hardening steels. In: 3rd European Conference Residual Stresses, Frankfurt am Ma German 4-6 November 1992; 1992.
[22] Henkisen M, Larson DB, Van Tyne CJ. On the analysis of distorsion and residual stress in carburized steels. J Eng Mater Technol 1992. 10.1115/1.2904186.
[23] Magnusson L, Ericsson T. Residual stress Load induced changes in carburised steel computations and experiments. Conference: "Residual stress and stress relaxation" Lake Placid, N.Y.; 1981 10.1007/978-1-4899-1884-0_3.
[24] Neu RW, Sehitoglu H. Transformation of retained austenite in carburized 4320 steel. Mettal Trans 1991. https://doi.org/10.1007/BF02667363.
[25] Lesage J, Chicot D, Elkaraishi M, Mesmacque G. Rôle d'un traitement de carbonitruration sur la résistance à la fatigue de l'acier 27MC5. MAT-TEC 1990 « technologie, comportement et traitement des matériaux; 1990. p 89-94.
[26] Ruckstuhl R, Martin M, Strat FLE. Influence du traitement thermochimique sur la mise en contrainte d'un matériau par grenaillage. TraitementThermique, No 1996; 292(1996):47–50.
[27] Jeddi D, Sidhom H, Ghiglione D, Lieurade H-P. Role of the cyclicstability of retained austenite in fatigue performance of carburized 14NiCr11 steel. J Mater Eng Performance 2005;14(1):37–49.
[28] Jeddi D, Sidhom H, Lieurade H-P, Ghiglione D. Rôle de l'austénite résiduelle dans la tenue en fatigue de l'acier 14NiCr11 cémenté. Traitement Thermique, janv-fev; 2005. p. 32–40.
[29] Jeddi D, Lieurade H-P. Effect of retained austenite on high cycle fatigue behavior of carburized 14NiCr11 steel. Proc Eng 2010;2(1):1927–36. https://doi.org/10.1016/j.proeng.2010.03.207.
[30] Qin S, Zhang C, Zhang B, Ma H, Zhao M. Effect of carburizing process on high cycle fatigue behavior of 18CrNiMo7-6 steel. J Mater Res Technol 2022;16:1136–49. https://doi.org/10.1016/j.jmrt.2021.12.074.
[31] Christodoulou PI, Kermanidis AT, Krizan D. Fatigue behavior and retained austenite transformation of Al-containing TRIP steels. Int J Fatigue 2016;91:220–31.
[32] Morris D, Sadeghi F, Singh K, Voothaluru R. Residual stress formation and stability in bearing steels due to fatigue induced retained austenite transformation. Int J Fatigue 2020;136:105610.
[33] Liu Z, Zhang S, Wang S, Feng Y, Peng Y, Gong J, et al. Redistribution of carbon and residual stress in low-temperature gaseous carburized austenitic stainless steel during thermal and mechanical loading. Surface Coat Technol 2021;426:127809.
[34] Zacconne MA, Krauss G. Fatigue and strain hardening of simulated case microstructures in carburized steels, in conference proceedings: Heat Treatment and Surface Engineering: New Technology and Practical Applications, Chicago, Illinois, USA, 28-30 Sept. 1998; 1998. p. 285-290.
[35] Dai Z, Chen H, Ding R, Lu Qi, Zhang C, Yang Z, et al. Fundamentals and application of solid-state phase transformations for advanced high strength steels containing metastable retained austenite. Mater Sci Eng R 2021;143:100590.
[36] Hossain R, Pahlevani F, Quadir MZ, Sahajwalla V. Stability of retained austenite in high carbon steel under compressive stress: an investigation from macro to nano scale. Sci Rep 2016. https://doi.org/10.1038/srep34958.
[37] Diego-Calderón Id, Rodriguez-Calvillo P, Lara A, Molina-Aldareguia JM, Petrov RH, De Knijf D, et al. Effect of microstructure on fatigue behavior of advanced high strength steels produced by quenching and partitioning and the role of retained austenite. Mater Sci Eng A 2015;641:215–24.
[38] Park HS, Han JC, Lim NS, Seol J-B, Park CG. Nano-scale observation on the transformation behavior and mechanical stability of individual retained austenite in CMnSiAl TRIP steels. Mater Sci Eng A 2015;627:262–9.
[39] Parrish G. The influence of microstructure on the properties of case-carburised components: Part 4. Heat Treat Met 1976;4:101–9.
[40] Inada A, Yaguchi H, Inoue T. The effects of retained austenite on the fatigue properties of carburised steels. The 8th International Congress on Heat Treatment of Materials. 1992.
[41] Theng G, Ooi C, Roy S, Sundararajan S. Investigating the effect of retained austenite and residual stress on rolling contact fatigue of carburized steel with XFEM and experimental approaches. Mater Sci Eng A 2018. https://doi.org/10.1016/j.msea.2018.06.078.
[42] Shen Yi, Moghadam SM, Sadeghi F, Paulson K, Trice RW. Effect of retained austenite – Compressive residual stresses on rolling contact fatigue life of carburized AISI 8620 steel. Int J Fatigue 2015;75:135–44.
[43] Qin S, Wang L, Di L, Zhang C, Zhao M. Effect of carburizing process on bending fatigue performance of notched parts of 18CrNiMo7-6 alloy steel. Eng Fail Anal 2023;147:107161.
[44] Xue Y, Yan Y, Yu W, Dong M, Shi J, Wang M. Microstructure and fatigue properties of 17Cr2Ni2MoVNb gear steel after gas carburizing and low-pressure carburizing. Int J Fatigue 2023;167:107314.
[45] Asi O, Can AÇ, Pineault J, Belassel M. The effect of high temperature gas carburizing on bending fatigue strength of SAE 8620 steel. Mater Des 2009;30(5):1792–7.
[46] Qin S, Zhang C, Zhang B, Ma H, Zhao M. Effect of carburizing process on high cycle fatigue behavior of 18CrNiMo7-6 steel[J]. J Mater Res Technol 2022;16:1136–49. https://doi.org/10.1016/j.jmrt.2021.12.074.
[47] Genel K, Demirkol M. Effect of case depth on fatigue performance of AISI 8620 carburized steel. Int J Fatigue 1999;21:207–12.
[48] Kim HJ, Kweon YG. High cycle fatigue behavior of gas-carburized medium carbon Cr-Mo steel. Metall Mater Trans A 1996. https://doi.org/10.1007/BF02652349.
[49] PRESTON (1991). Effect of steelmaking route on the bending fatigue strength of carburizing steel SS2506. MD-vol.28, Impact of Improved Material Quality on Properties, Product Performance, and design, ASME 1991. p.15-26.
[50] Wyszkowski J, Priegnitz H, Gozdzik E, Ratkiewicz A. Influence de l'austénite résiduelle sur quelques propriétés de l'acier cémenté. Revue de Métallurgie, Juin 1971;68(6):411–22.
[51] Lesage J, Iost A. Influence de l'austénite résiduelles sur la durée de vie en fatigue d'aciers carbonitrurés, C.R.Acad.Sc., Paris, France, tome 305. Série 1987;II:77–80.
[52] Grosch J, Schwarz O. Retained austenite and residual stresses distribution in deep cooled carburized microstructures. Second international conference on carburising and nitriding with atmospheres. 1995.
[53] Kim C, Diesburg DE, Eldis GT. Effect of residual stress on fatigue fracture of case-hardened steels-An analytical Model. Conference: " Residual stress effects in fatigue". 1981.
[54] Zürn J, Razim C, Grosch J.The effect of residual stress in case hardening. Conference: "Heat Treatment and Surface Engineering: New Technology and Practical applications", Chicago, Illinois USA; 1988.
[55] Abareshi M, Emadoddin E. Effect of retained austenite characteristics on fatigue behavior and tensile propertiesof transformation induced plasticity steel. Mater Des 2011;32(10):5099–105.
[56] Umino M. Fatigue strength of surface hardened 4100S steel. MPR, April 1987. p. 295–296.
[57] Dament A, Elhaik R, Lafont R, Wyss R. Tenue en fatigue superficielle des couches carbonitrurées et cémentées en relation avec la répartition des contraintes résiduelles et les modifications du réseau cristallin apparaissant en cours de fatigue. Traitement Thermique, no 1974;87(1974):87–97.
[58] Michiuchi M, Nambu S, Ishimoto Y, Inoue J, Koseki T. Relationship between local deformation behavior and crystallographic features of as-quenched lath martensite during uniaxial tensile deformation. Acta Materialia 2009. https://doi:10.1016/j.actamat.2009.06.021.
[59] Terres MA, Laalai N, Sidhom H. Effect of nitriding and shot-peening on the fatigue behavior of 42CrMo4 steel: experimental analysis and predictive approach. Mater Des 35, https://doi:10.1016/j.matdes.2011.09.055.
[60] Peterson RE. Stress concentration factors. J. Wiley and Sons. Wiley-Interscience, New-York; 1974.
[61] Convert F, Miege B. De bonnes raisons de doser l'austénite. Traitement Thermique 1997;301:40–5.
[62] Moore MG, Evans WP. Mathematical correction for stress in removed layers in X-ray diffraction residual stress analysis. SAE Trans 1958;66:340–5.

[63] Lasserre S, Lizarazu F, Seguret J. Machine d'essais de fatigue des matériaux sous sollicitations combinées et éprouvette fixe. Brevet d'invention 77-37146 (ENSAM Bordeaux); 1977.
[64] Wang Y. Etude et modélisation de l'effet du revenu sur les évolutions des microstructures, ducomportement thermomécanique et des contraintes résiduelles de trempe. InstitutNationalPolytechnique de Lorraine. Français. NNT: 2006INPL047N; 2006.
[65] Kang T, Zhao Z, Liang J, Guo J, Zhao Y. Effect of the austenitizing temperature on the microstructure evolution and mechanical properties of Q&P steel. Mater Sci Eng A 2020. https://doi.org/10.1016/j.msea.2019.138584.